Green Chemistry

PAPER

View Article Online
View Journal

Cite this: DOI: 10.1039/d6gc00387g

Enhancing multi-enzymatic CO_2 conversion *via* reactor engineering: effects of mass transfer on sustainable and green metrics

Sady Roberto Rodriguez, Marina Guillén and Oscar Romero *

The global energy transition toward decarbonization requires highly efficient Carbon Capture and Utilization (CCU) technologies that combine economic feasibility, operational stability and environmental sustainability. A key factor for successful CCU is efficient CO_2 gas–liquid transfer, which can be optimized through tailored reactor designs to maximize yields and utilization. Technological advances such as CO_2-specific sensors have enabled accurate monitoring of CO_2 mass balance enhancing the efficiency of its conversion. This work addresses an in-depth analysis of CO_2 mass transfer in a stirred-tank reactor, focusing on the impact of volumetric gas flow rate on gas–liquid transfer during the multi-enzymatic conversion of CO_2 into high-value compounds using a co-immobilized biocatalyst of formate dehydrogenase and glycerol dehydrogenase enzymes. The volumetric mass transfer coefficient (k_La) was determined at different gas flow rates (1, 0.5 and 0.1 vvm) from a 24% CO_2 gas mixture, with the reaction carried out at 0.1 vvm achieving an outstanding formate production of 66.1 ± 1.4 mM (3 g L^{-1}), due to near-neutral pH conditions that improved the reaction conditions and enhanced biocatalyst stability by at least 1.8-fold compared with high gas flow rate (1.0 vvm). Furthermore, a remarkable CO_2 capture efficiency of 93.3 ± 2.1% was achieved at 0.1 vvm, along with a high selectivity toward formate and glycerol carbonate, reflecting a complete CO_2 conversion into target products. Finally, the environmental impact of the reaction at 0.1 vvm showed a lower contribution to climate change, reaching 13.2 kg CO_2 eq. per kg products. These results underscore enzymatic CO_2 reduction as an effective and sustainable approach for the development of bio-based industrial processes with a markedly reduced environmental footprint.

Received 20th January 2026,
Accepted 22nd March 2026

DOI: 10.1039/d6gc00387g

rsc.li/greenchem

Green foundation

1. This work advances green chemistry as the first enzymatic Carbon Capture and Utilization (CCU) report using environmental metrics to support carbon-neutral manufacturing. It valorises industrial emissions and renewable feedstocks into high-value chemicals, significantly reducing the environmental footprint for climate change.
2. The system achieved a record 66.1 mM formate production, 93.3% capture efficiency, and complete conversion into high-value products. This achievement demonstrates high process selectivity and a remarkably low Global Warming Potential (GWP) of 13.2 kg CO_2 eq. per kg of product.
3. Future work should focus on: (1) optimizing FDH catalytic efficiency (k_{cat}/K_m) *via* protein engineering or bioprospecting to overcome kinetic bottlenecks, and (2) enhancing CO_2 mass transfer through synergy with Carbonic Anhydrase (CA).

1. Introduction

Carbon dioxide (CO_2) is gaining increasing recognition as a valuable carbon feedstock as the global energy landscape shifts toward decarbonization. In this context, CO_2 conversion technologies offer a strategic approach to simultaneously enhance energy storage, contribute to global climate objectives, and promote the development of a circular carbon economy.[1] However, scaling up these technologies to industrial processing plants requires comprehensive optimization to ensure economic viability and operational stability.[2] Despite significant advances to develop more efficient catalysts for CO_2 reduction and translating these processes to larger scales, studies focusing on reactor engineering aspects to optimize these catalytic processes remain limited.[3]

For conventional chemical reactions, including catalytic conversions, reactor engineering has long provided a robust and effective framework for achieving maximum productivity while minimizing cost and energy losses.[4] Moreover, this approach is crucial for enhancing reaction performance, facili-

Bioprocess Engineering and Applied Biocatalysis Group, Department of Chemical, Biological and Environmental Engineering, Universitat Autònoma de Barcelona, 08193 Bellaterra, Catalonia, Spain. E-mail: Oscar.Romero.Ormazabal@uab.cat

tating efficient mass and heat transfer, improving product selectivity and increasing overall process efficiency.[4,5] Under these principles, a fundamental requirement for the success of both CO_2 capture and utilization processes is the efficient transfer from the gas to the aqueous phase, enabling effective mitigation.[6] Therefore, evaluating CO_2 mass transfer through tailored reactor configurations is essential to advance industrial deployment of CCU technologies.

Under this context, the volumetric mass transfer coefficient (k_La) is a key parameter that quantifies the rate of gas movement to the liquid phase, directly influencing reaction kinetics and overall performance in inter-phase systems. k_La is commonly used to assess reactor efficiency, optimize the design and operation of mixing and sparging equipment, and plays a critical role in process scale-up.[7] In many processes involving the direct conversion of gases such as CO_2 or oxygen (O_2), mass transfer may be slower than the reaction rate; therefore, the rate of gas–liquid transfer becomes the limiting step of the entire process, and its optimization is therefore crucial.[8] Furthermore, in the case of CO_2 there is an additional step during this transfer, the chemical reaction rate at which CO_2 reacts with water to form various inorganic carbonate species in equilibrium.[9] Therefore, assessing the volumetric mass transfer coefficient of CO_2 in the biocatalytic reaction is crucial for evaluating reaction rates, improving process efficiency, optimizing reactor performance and enabling successful scale-up.

CO_2 gas–liquid transfer has been typically considered as analogous to O_2 transfer by applying correction factors to account for differences in diffusion coefficients between the two gases.[10] This approach stems from the extensive availability of O_2 sensors, the ease of measuring O_2 transfer, and the abundance of published data.[11] However, modern advances have enabled the development of CO_2-specific sensors that directly measure gas–liquid transfer by detecting pH changes caused by inorganic carbon species,[7] as the digital in-line CO_2 sensor used in this work. In addition, most CO_2 mass-transfer studies have focused on low pH conditions, where its equilibrium concentration is higher, while only few have evaluated its k_La at neutral or higher pH.[12]

Consequently, by applying mass transfer analysis and reactor engineering principles, it is possible to integrate instrumentation such as sensors and control systems that generate reliable data to evaluate the overall process balance, ensuring favorable economics when all reactor components perform optimally. Furthermore, adjusting the gas supply rate to maintain the dissolved CO_2 concentration near the optimum for the reaction conditions can reduce unnecessary gas expenditure and maximize the fraction effectively converted into product.[13]

In this study, we investigate the mass transfer of CO_2 in a multi-enzymatic reduction system for the simultaneous production of three high value-added compounds: formate, dihydroxyacetone (DHA) and glycerol carbonate (GC) (Fig. 1). In our previous work, the multi-enzymatic system was developed using the enzymes formate dehydrogenase (FDH) and glycerol dehydrogenase (GlyDH) in their free form,[14] as well as co-immobilized on the Ni^{2+}-ReliZyme carrier (bifunctional biocatalyst).[15] FDH enzyme has been considered a key model for the design of CO_2 fixation systems, enabling the production of the only CO_2-derived product currently manufactured at industrial scale, formic acid or formate.[16] This compound finds a wide range of industrial applications, serving as a chemical feedstock, in the textile and leather industries, and as a food additive.[17] To complement this reaction, GlyDH was selected to enable *in situ* cofactor regeneration through glycerol valorization, which is abundantly generated as a byproduct of the bio-

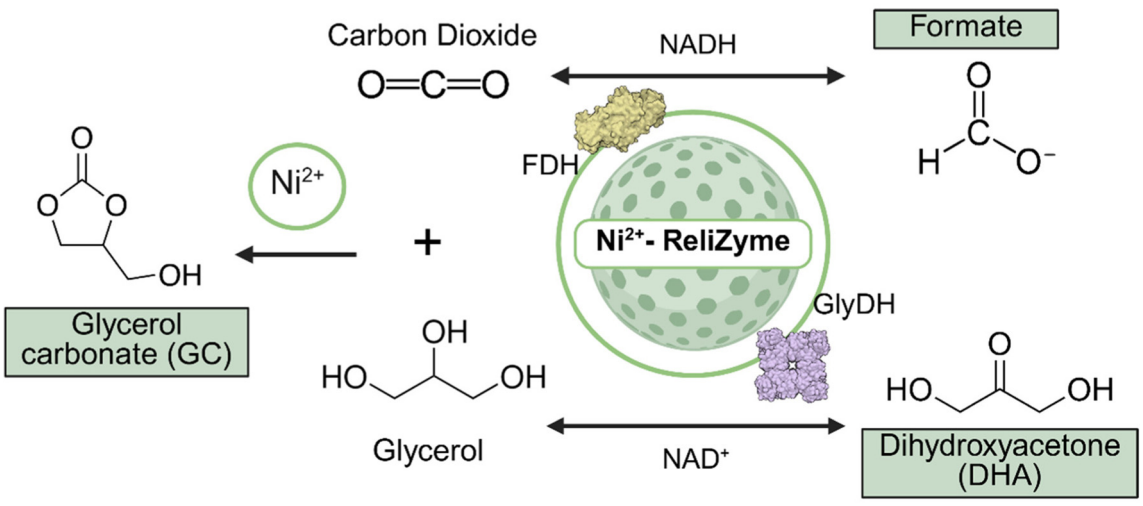

Fig. 1 Overview of the multi-enzymatic system for CO_2 reduction to high-value compounds. The co-production of formate and DHA – from CO_2 and glycerol – is enzymatically catalyzed by formate dehydrogenase (FDH) and glycerol dehydrogenase (GlyDH) enzymes co-immobilized on the Ni^{2+}-ReliZyme carrier, allowing the *in situ* NADH regeneration. Likewise, the synthesis of the by-product glycerol carbonate (GC) from CO_2 and glycerol is catalyzed by the nickel (Ni^{2+}) present in the bifunctional biocatalyst (prepared on Ni^{2+}-ReliZyme carrier) and zinc (Zn^{2+}) in the active site of GlyDH from *Bacillus stearothermophilus*.

diesel industry, making it an industrially relevant and low-cost feedstock.[18] From this, DHA is produced, a compound utilized as a tanning agent in the cosmetic industry and as a building block in pharmaceutical synthesis.[19] This FDH–GlyDH synergy has ensured efficient NADH cofactor recycling while simultaneously coupling two thermodynamically challenging reactions and adding value to industrial feedstocks like CO_2 and glycerol.[14] Additionally, GC is formed as a byproduct through the direct carboxylation of CO_2 and glycerol[20] [reaction mechanism in Fig S2, SI], catalyzed by metals such as nickel (Ni^{2+}) on the immobilization carrier and zinc (Zn^{2+}) in the active site of metalloenzyme GlyDH from *Bacillus stearothermophilus*.[21] This is another high-value chemical with applications in the polymer, pharmaceutical, and cosmetic industries, as well as a versatile intermediate in green chemistry and sustainable synthesis.[20]

For this work, through reactor engineering, the setup of the multi-enzymatic reaction enabled the development of a mass balance to quantify CO_2 captured and converted at different gas flow rates using an *in situ* sensor system. Likewise, the environmental impact of this bioprocess was assessed through its contribution to climate change (GWP: Global Warming Potential). These findings represent a novelty in the study of CO_2 mass transfer in biocatalytic processes and provide a framework to support the development of sustainable and environmentally friendly systems that combine the capture of CO_2 gas emissions and their subsequent conversion into valuable compounds in a single step.

2. Experimental

2.1. Materials

All reagents were purchased from Sigma Aldrich® (St Louis, MO, USA) and PanReac Quimica S.L.U. (Barcelona, Spain). The cofactors NADH and NAD^+ were purchased from GERBU Biotechnik GmbH (Heidelberg, Germany). ReliZyme™ EP403S resin was purchased from Resindion S.r.l. (Binasco, Italy). All samples and buffers were prepared in Milli Q water (18.2 MΩ cm, Merck Millipore, USA). The gas mixture 24% CO_2 and 76% N_2 was obtained from Carburos Metalicos (Barcelona, Spain). Formate dehydrogenase (EC 1.17.1.9) and glycerol dehydrogenase (EC 1.1.1.6) enzymes were produced and purified by the research group according to the procedures reported by the authors.[14]

2.2. Determination of the CO_2 volumetric mass transfer coefficient (k_La)

The volumetric mass transfer coefficient (k_La) for CO_2 was determined in a stirred-tank reactor (SpinChem, Sweden) with 200 mL of phosphate buffer 100 mM (pH 7.5) as reaction medium, temperature of 30 °C and stirring set at 300 rpm. A gas mixture composed of 24% CO_2 in nitrogen, similar to the off-gases composition from blast furnaces in the iron and steel industry (24.5% CO_2)[22] was employed. The dissolved CO_2 concentration was monitored using a digital in-line CO_2 sensor InPro5000i/12/220 (Mettler Toledo S.A.E., Barcelona, Spain). This sensor was immersed in the liquid at the same depth for all experiments and the data was collected by an Analytical Transmitter M400 Type 3 (Metter Toledo S.A.E., Barcelona, Spain). The volumetric gas flow rate per volume of liquid per minute (vvm) was assessed at 0.1, 0.5, 1.0, and 1.5 vvm. Additionally, the effect of the immobilization carrier (Ni^{2+}-ReliZyme) resuspended in the medium was evaluated by applying loadings of 5%, 10%, 15%, and 20% of the total reaction volume. Sensor response time was assessed by equilibrating the CO_2 concentration in the medium and then transferring the sensor to a CO_2-free medium, according to the equation in section S5 in the SI. The k_La was calculated using the following equation, applying a nonlinear model with the Solver tool (Microsoft ® Excel):

$$C_{mes} = C^* + \frac{C^* - C_0}{1 - \tau k_L a}\left[\tau k_L a \exp\left(-\frac{t}{\tau}\right) - \exp(-k_L a t)\right] \quad (1)$$

where: C_{mes}: CO_2 concentration measured by the sensor at certain time t; C^*: equilibrium or saturation CO_2 concentration in the liquid phase; C_0: initial dissolved CO_2 concentration in the medium; k_La: the volumetric mass transfer coefficient (min^{-1}); τ: sensor response time; t: time at which the CO_2 concentration is measured.

2.3. Multi-enzymatic reduction of CO_2 by assessing different volumetric gas flow rates

The multi-enzymatic reduction of CO_2 was performed in a stirred-tank reactor using a co-immobilized bifunctional biocatalyst, with *in situ* NADH regeneration and continuous gas supply. As reaction medium, phosphate buffer 100 mM (pH 7.5) was used with NADH 1 mM, glycerol 100 mM, and gas continuously bubbled at volumetric flow rates of 0.1, 0.5, and 1 vvm from a gas mixture with 24% CO_2 in nitrogen, using a mass flow controller EL-FLOW (Bronkhorst, Netherlands). A total of 20 g of biocatalyst (containing approximately 40 mg g^{-1} of GlyDH and 10 mg g^{-1} FDH) were suspended in 200 mL of reaction medium. The preparation of this biocatalyst is detailed in SI (section S1).

To monitor the CO_2 inlet and outlet of the reactor, two BCP-CO_2 gas analyzers were installed for *in situ* CO_2 measurements (measured every 5 min). The data were collected and analyzed using the BlueVis software. (BlueSens GmbH, Germany). A digital in-line CO_2 sensor InPro5000i/12/220 was also incorporated to measure its dissolved concentration (measured every 2 min) and the data was collected by an Analytical Transmitter M400 Type 3 (Metter Toledo S.A.E., Barcelona, Spain). Additionally, a Syntrode pH electrode, connected to a 916 Ti-Touch titrator (Metrohm Hispania, S.L.U, Spain), was installed to continuously monitor the pH throughout the reaction, measuring every hour. Fig. 2 shows the full flow diagram of the reaction setup with the sensors involved. The experiments were conducted in duplicate at 30 °C with constant stirring at 300 rpm over 80 h. Samples were taken

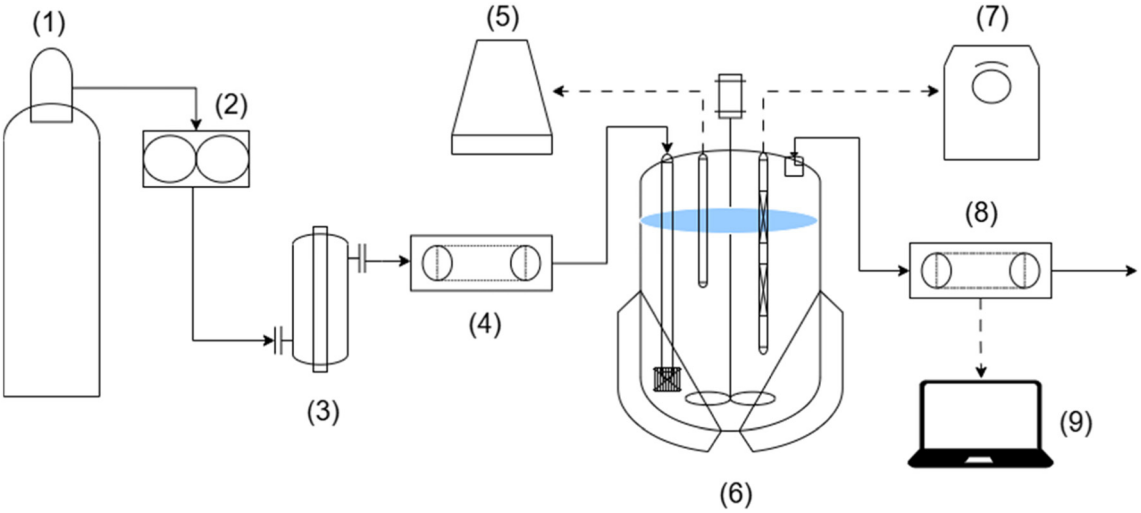

Fig. 2 Flow diagram of the setup for the multi-enzymatic reduction of CO_2 to high value chemicals. (1) Gas mixture 24% CO_2 in N_2. (2) Gas flowmeter. (3) Gas humidification. (4) CO_2 input sensor. (5) pH-Monitoring titrator. (6) Stirred-tank reactor. (7) Dissolved CO_2 analytical transmitter. (8) CO_2 output sensor. (9) Gas sensor data collection and analysis. (—) Continuous gas flow. (---) Data collection.

periodically to analyze substrate and product concentrations, as well as enzyme activity (sections S2 and S4, SI).

2.4. CO_2 mass balance analysis

The mass balance of CO_2 during the reaction was determined through the sensor-based system integrated into the experimental setup previously detailed. First, the amount of CO_2 at the inlet and outlet of the reactor per unit of time (h) was calculated following eqn (S2) and (S3). Accordingly, the mass of CO_2 captured was calculated using the following equation:

$$CO_2\ \text{captured}\ (\text{g h}^{-1}) = CO_2\ \text{inlet}\ (\text{g h}^{-1}) - \ CO_2\ \text{outlet}\ (\text{g h}^{-1}) \quad (2)$$

Afterwards, the total amount of CO_2 (in g) that entered the reactor and the amount captured throughout the reaction were calculated by estimating the area under the curve according to eqn (S4) in SI.

For CO_2 converted to formate and glycerol carbonate (GC), only the fraction of CO_2 atoms incorporated into each product was considered. As reported by Gao *et al.*,[23] all CO_2 atoms participate in forming the linear carbonate intermediate during glycerol carbonate synthesis, as well as in formate synthesis. Therefore, correction factors were calculated based on the molecular weights of CO_2 and each product, as described by eqn (S5) in SI. These factors were then incorporated into the subsequent equation to determine the mass of CO_2 converted into product:

$$CO_2\ \text{converted}\ (\text{g}) = \text{amount of product}\ (\text{g}) \times \text{CF} \quad (3)$$

where: CF formate = 0.978; CF glycerol carbonate = 0.373.

The total amount of CO_2 converted corresponds to the sum of the CO_2 incorporated into each product.

The product yields obtained per g of CO_2 captured were calculated based on the total mass of each molecule produced and expressed as g g^{-1} (dimensionless). The following equation was employed:

$$\text{Product yield}\ (\text{g g}^{-1}) = \frac{\text{total mass of formate or GC produced (g)}}{\text{mass of } CO_2 \text{ captured (g)}} \quad (4)$$

Finally, two CO_2 conversion performance metrics commonly employed in the green chemistry were considered. First, process selectivity refers to the system's ability to direct captured CO_2 toward the desired product, reflecting the reaction efficiency under the given conditions. The following equation was applied:

$$\text{Selectivity}\ (\%) = \frac{\text{moles product (formate or GC)}}{\text{moles } CO_2 \text{ captured}} \times 100 \quad (5)$$

The sum of the selectivity toward each product represents the global process selectivity.

On the other hand, carbon efficiency indicates how effectively carbon introduced into a process is incorporated into the final product, accounting indirectly for losses in by-products or emissions and providing a key measure of process sustainability and economic efficiency. The carbon efficiency equation used in this work was adapted from Belsa *et al.*[24] and Constable *et al.*,[25] indicating the sum of the yields of the final CO_2-derived products, formate and glycerol carbonate (GC):

$$\text{Carbon efficiency} = \frac{\sum C_x n_x}{n_{CO_2}} \times 100 \quad (6)$$

where C_x = number of carbons from CO_2 in each product x (one single carbon); n_x = number of moles of each product (formate or GC); n_{CO_2} = number of moles of CO_2 that entered the system.

2.5. Environmental impact assessment

To assess the environmental impact of this process on climate change, the global warming potential (GWP) was determined for each reaction performed at different volumetric flow rates. The GWP was calculated based on the product mass (eqn (7)) and the energy consumed (eqn (8)), following the equations proposed by Domínguez de María:[26]

$$\mathrm{GWP\,(water(wwtp))} = \frac{0.073 \times \%\mathrm{water\,treated}}{\mathrm{conv.} \times [\mathrm{SL}]} \quad (7)$$

$$\mathrm{GWP\,(water(energy))} = \left(\frac{0.037 \times \Delta T}{\mathrm{conv.} \times [\mathrm{SL}]}\right) + t\left(\frac{0.0056 \times \Delta T}{\mathrm{conv.} \times [\mathrm{SL}]}\right) \quad (8)$$

where: wwtp = wastewater treatment plant; conv.: CO_2 conversion (%); [SL]: product concentration expressed in kg L^{-1}. t: reaction time (80 h).

Considerations: 100% of the residual water was assumed to be treated in a WWTP. Room temperature was set at 25 °C.

3. Results and discussion

3.1. Determination of the volumetric mass transfer coefficient (k_La) of CO_2 in a stirred-tank reactor

To study CO_2 mass transfer, its volumetric mass transfer coefficient (k_La) was determined in the stirred-tank reactor used for the multi-enzymatic CO_2 reduction reaction. Estimating k_La for CO_2 is crucial in bioreactor design, as it assesses reactor efficiency and guides scale-up, especially in processes requiring continuous CO_2 supply, such as in several chemical processes and in some fermentations.[27] Moreover, optimizing CO_2 transfer also reduces costs by supplying only the necessary gas amount, thereby improving resource efficiency.[28] However, understanding CO_2 chemical equilibrium in water is essential to evaluate its mass transfer in aqueous systems. CO_2 interacts with water to form carbonic acid, bicarbonate, and carbonate, following this dissociation equilibria at pH 7.0 and 30 °C:[29]

$$CO_2 + H_2O \leftrightarrow H_2CO_3$$

$$H_2CO_3 \leftrightarrow H^+ + HCO_3^- \quad (K_1 = 4.3 \times 10^{-7}, \mathrm{p}K_1 = 6.37)$$

$$HCO_3^- \leftrightarrow H^+ + CO_3^{2-} \quad (K_2 = 5.6 \times 10^{-11}, \mathrm{p}K_2 = 10.25)$$

According to some reports, the Total Inorganic Carbon (TIC), which reflects the distribution of these species as a function of the medium's pH, is a key parameter for studying CO_2 gas–liquid transfer, since it not only estimates the amount of CO_2 absorbed but also identifies the dominant form in which it is present.[12] This parameter can be determined using conventional methods such as alkalinity titration or specialized techniques like Non-Dispersive Infrared (NDIR) analysis.[30] However, in this study, $k_La_{(CO_2)}$ was determined using a dynamic method that requires continuous real-time tracking of the dissolved CO_2 concentration. For that, a digital in-line CO_2 sensor was employed, which measures only dissolved CO_2 (mg L^{-1}). This provides a simplified methodology and enables immediate *in situ* tracking of concentration changes, which are essential for the accurate and rapid determination of k_La throughout the process. The operating principle of this sensor, based on the Severinghaus principle, is illustrated in Fig. S1 in SI.

In general, k_La determination depends on reactor type and volume, operating conditions (temperature, pH, pressure, agitation), flow rate, immersion depth, suspended solids and the properties of the gas and liquid phases, among other factors.[31] In this work, the agitation speed was set at 300 rpm to prevent biocatalyst damage at higher stirring rates. Consequently, other factors such as gas flow rate and resuspended solids (immobilization carrier), were examined. As an initial step, the response time of the dissolved CO_2 sensor (τ) was assessed according to eqn (S1) in SI. Fig. S3 in the SI provides a graphical illustration and a brief discussion of the sensor's response to a CO_2-free medium, yielding a response time of 0.93 min (56 s).

Fig. 3 shows the $k_La_{(CO_2)}$ values obtained by evaluating different volumetric flow rates of the 24% CO_2 mixture, along with the immobilization carrier (Ni^{2+}-ReliZyme) present at 10% of the total volume are plot. As expected, the CO_2 gas–liquid transfer rate increased with the volumetric flow rate from 0.1 to 1 vvm, while no further increase was observed at 1.5 vvm, indicating that the mass transfer limit had been reached (Fig. 3A). In experiments with 10% resuspended carrier, $k_La_{(CO_2)}$ increased compared to assays without carrier, particularly at higher flow rates such as 1 vvm (Fig. 3A). Suspended solids likely enhance gas–liquid transfer by increasing turbulence and dispersing gas bubbles, expanding the surface area for solubilization.[32] As before, no further increase was observed at 1.5 vvm.

Table S1 in the SI summarizes the parameters evaluated for $k_La_{(CO_2)}$ in the experiments described. Across flow rates from 0.1 to 1 vvm, the data were well described by a linear model ($R^2 > 0.99$). Under these conditions, a CO_2 gas–liquid transfer rate of 7.35 ± 0.44 mg L^{-1} min^{-1} (0.17 ± 0.02 mM min^{-1}) was achieved with 10% resuspended carrier at 1 vvm. The $k_La_{(CO_2)}$ was also determined with pure CO_2. As expected, a highest transfer rate was observed, yielding a k_La of 0.32 ± 0.03 min^{-1} (10.75 mg L^{-1} min^{-1}, Table S1), due to the higher partial pressure driving faster gas–liquid transfer.

Finally, varying the resuspended carrier at 1 vvm (Fig. 3B) showed that concentrations above 10% caused a linear decrease in $k_La_{(CO_2)}$, likely due to interface saturation and increased fluid viscosity limiting bubble mobility.[33] Minimal differences were observed between 5% and 10%, suggesting a negligible effect within this range. Hence, a carrier concentration in that range (from 10–20%) and volumetric flow rate from 0.1–1.0 vvm from the gas mixture 24% CO_2 may represent the optimal operating conditions for this multi-enzyme system.

Compared to oxygen (O_2), for which k_La is typically measured, CO_2 generally has a lower k_La under standard conditions (25 °C and 1 atm). Under similar reaction conditions in this same reactor, $k_La_{(O_2)}$ can reach values up to an order of

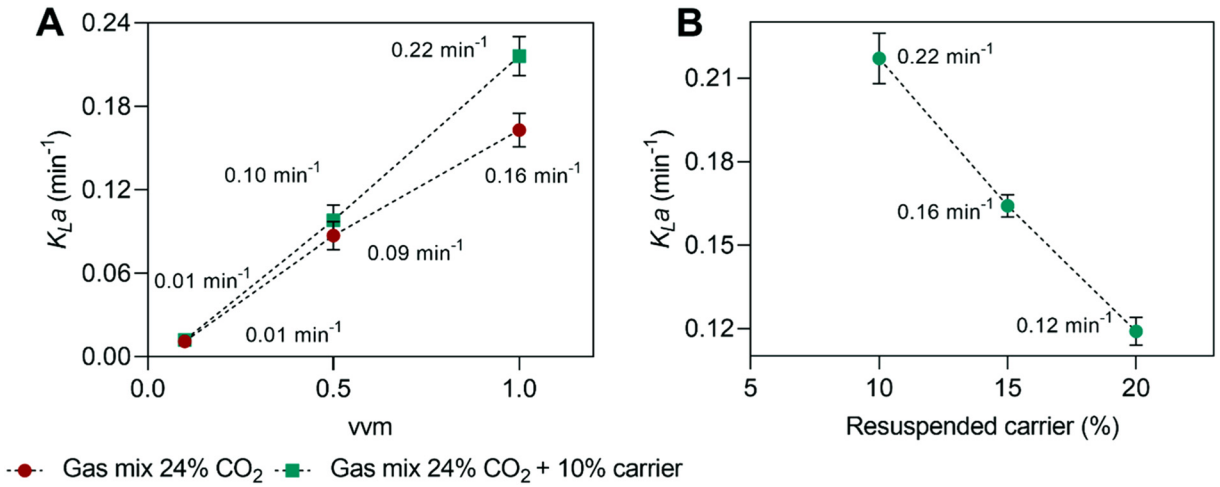

Fig. 3 (A) Gas–liquid CO_2 transfer rate (k_La) by varying the volumetric flow rate (vvm) from the gas mixture 24% CO_2 in nitrogen and with a fixed amount of suspended carrier in the liquid (10%). (B) Gas–liquid CO_2 transfer rate (k_La) by varying the percentage of resuspended Ni^{2+}-ReliZyme in the medium at 1 vvm from the gas mixture 24% CO_2.

magnitude higher than $k_La_{(CO_2)}$ when air is directly bubbled into the system. Although CO_2 is more soluble than O_2 in water (0.033 *vs.* 0.001 mol L^{-1}) under standard conditions,[34] this results not only from physical dissolution but also from chemical interactions forming inorganic species that prolong CO_2 retention.[7] However, despite its higher solubility, CO_2 diffuses more slowly than O_2 due to its larger molecular size, and chemical reactions that reduce the free CO_2 available for transfer, leading to lower $k_La_{(CO_2)}$ values.[35]

In contrast, O_2 transfer is often limited by agitation, as increased stirring produces smaller bubbles and greater gas–liquid contact. In the case of CO_2, its transfer is also limited by agitation, but even more so by the gas flow rate, as higher flow rates continuously renews the gas–liquid concentration gradient, thereby enhancing mass transfer and leading to higher $k_La_{(CO_2)}$ values.[36] However, at lower flow rates, mass transfer is slower, but rapid gas saturation is avoided, maintaining the concentration gradient longer and allowing more efficient gas utilization. In addition, gas bubbles also remain in contact with the liquid for a longer time, promoting more effective CO_2 utilization.[7,37] Although some studies suggest estimating $k_La_{(CO_2)}$ by multiplying $k_La_{(O_2)}$ by 0.91 attributed to physicochemical differences,[38] these gases have demonstrated different diffusion coefficients, so their transfer and absorption kinetics can differ even when bubbled together.[39] However, in this study, $k_La_{(CO_2)}$ was successfully determined in a stirred-tank reactor using a potentiometric sensor, enabling accurate and reliable measurements.

Importantly, this study of gas–liquid mass transfer provides a foundation for potentially incorporating key parameters into reactor-scale simulations for dynamic mass balance and reaction kinetics modeling. The measured k_La values describe CO_2 transfer, allowing prediction of dissolved CO_2 profiles as a function of operating variables. These results pave the way for implementing gas–liquid mass transfer studies in other enzymatic CO_2 transformation including lactic acid production[22] and carboxylation, where reaction kinetics depend strictly on CO_2 mass transfer and pH levels Furthermore, this approach can be extended to other enzymatic processes involving gaseous substrates, such as oxidation reactions, which rely on maintaining optimal dissolved oxygen concentrations in the reaction medium.

3.2. Multi-enzymatic CO_2 reduction by evaluating different gas volumetric flow rates

The multi-enzymatic reduction of CO_2 into high-value compounds was assessed in a stirred-tank reactor by testing different volumetric flow rates (0.1, 0.5, and 1.0 vvm) of a gas mixture containing 24% CO_2, which corresponds to the typical CO_2 content reported for the off-gases from blast furnaces in the iron and steel industry.[22] Although the effect of different immobilization carrier loadings on the determination of $k_La_{(CO_2)}$ was also evaluated, a 10% carrier-to-volume ratio was used in all these following reactions to ensure good distribution of the carrier in the liquid and to avoid the effect of excessive solids on CO_2 gas–liquid mass transfer. The concentrations of both enzymes (GC-GlyDH and FDH) in the biocatalyst were previously optimized by the authors, for both their free[14] and co-immobilized on Ni^{2+}-ReliZyme forms.[15]

As a first point of comparison, it is important to understand the strong relationship between CO_2 flow rate and the pH resulting in the reaction medium. As previously explained, CO_2 reacts with water to form carbonic acid, which partially dissociates, releasing protons (H^+) and thereby modulating the pH of the medium.[40] Therefore, higher CO_2 flow rates lead to increased CO_2 mass transfer rate and a more pronounced decrease in pH compared to lower flow rates. However, this close relationship is also influenced by key factors in the reaction medium, including buffer capacity, temperature and partial pressure.[41] Fig. S4 in SI shows a comparison of pH evol-

ution over time for reactions at different vvm. At 1 vvm, the pH dropped sharply from 7.5 to 6.7 within one hour, then stabilized around pH 6.6. At 0.5 vvm, pH felt from 7.5 to 6.9 within one hour, then gradually to pH 6.7. At 0.1 vvm, the initial drop was minor, decreasing slowly from pH 7.3 to 7.0. Thus, the CO_2 dissolution rate governs pH changes over time, indicating that the three reactions occurred at different pH levels, which could potentially affect the reactions' microenvironment. Notably, accounting for the CO_2–carbonate equilibrium is also essential for accurately predicting dissolved CO_2 concentrations as a function of medium pH, mass transfer rate and other operating parameters, particularly when extrapolating these effects to potential reactor-scale simulations. This approach has previously been validated for the development of mass transfer models, highlighting gas flow rate and CO_2 loading as the key factors influencing the mass transfer rate[42] as well as for models based on mechanistic enzymatic kinetic models, such as those describing carbonic anhydrase, under a range of operating conditions including temperature, CO_2 partial pressure and concentration.[43,44]

Regarding the multi-enzymatic CO_2 conversion reaction, Fig. 4 presents the concentrations of formate, DHA, and glycerol carbonate, along with glycerol conversion, obtained after 80 h of reaction for the three evaluated volumetric flow rates. The time courses of the three reactions are illustrated in Fig. S5 (SI). As observed, a linear correlation ($R^2 > 0.99$) was found between the gas volumetric flow rate and each product concentrations, as well as glycerol conversion across all experiments, suggesting that CO_2 input and its concentration in the medium are key factors for the performance and efficiency of this multi-enzymatic system. Formate production was inversely proportional to CO_2 input, with lower flow rates resulting in

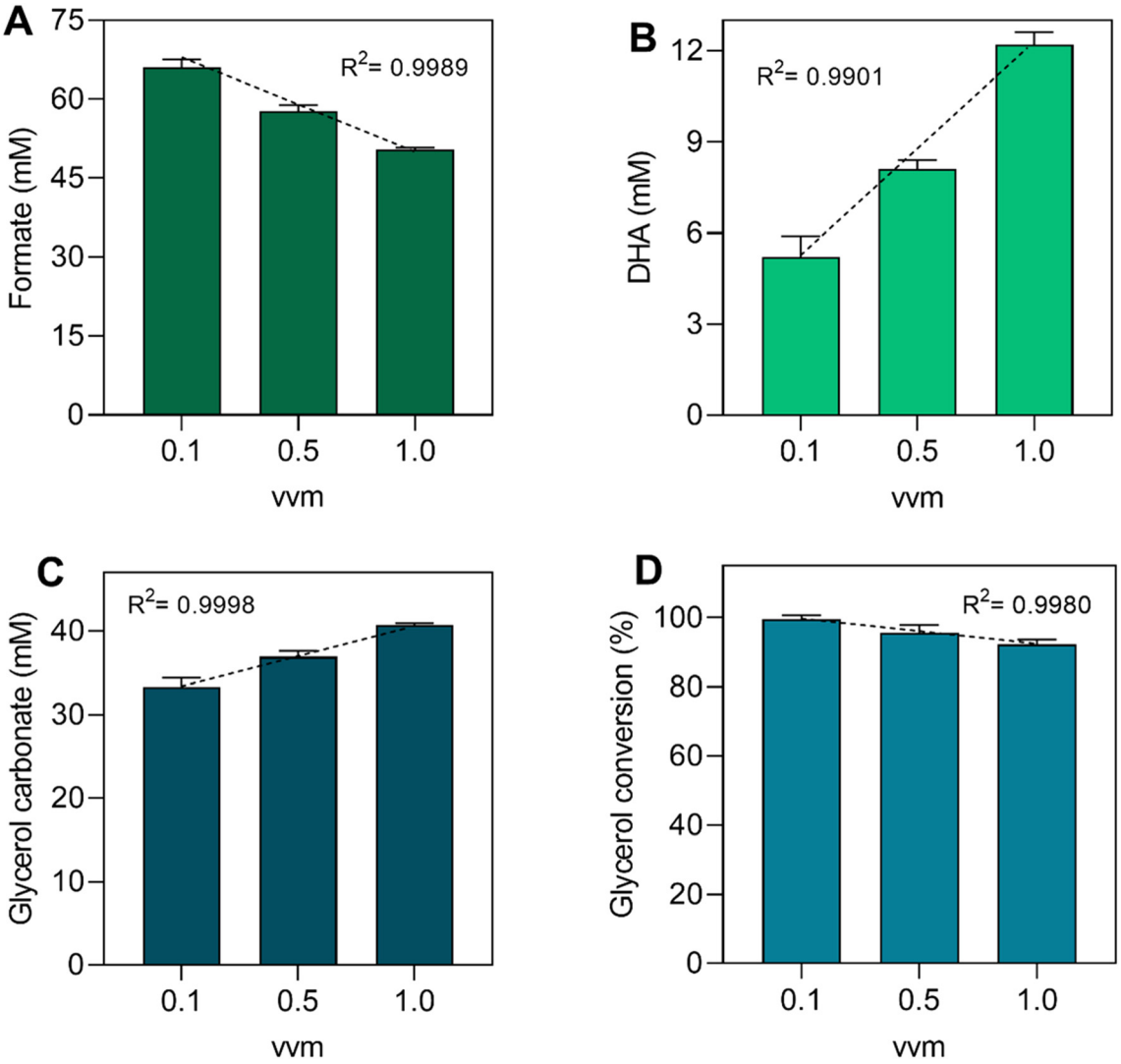

Fig. 4 Multi-enzymatic reduction of CO_2 to high-value compounds using a bifunctional co-immobilized biocatalyst with *in situ* cofactor regeneration, evaluating three different gas volumetric flow rates from a 24% CO_2 gas mixture. (A) Formate [mM]. (B) DHA [mM]. (C) Glycerol carbonate [mM]. (D) Glycerol conversion [%]. The DHA concentrations shown in this figure correspond only to the soluble fraction (not adsorbed onto the biocatalyst).

higher concentrations (Fig. 4A). At the lowest flow rate (0.1 vvm), and therefore at a pH closer to neutral (pH 7.0), the highest formate concentration was achieved, 66.1 ± 1.4 mM (equivalent to 3 g L^{-1}). This represents a 31.2% increase compared to the reaction conducted at 1 vvm (50.4 ± 0.3 mM). This result represents up to an 8.5-fold improvement over previous reports on enzymatic CO_2 reduction and cofactor regeneration platforms.[45–47] Similarly, this formate production is comparable to electrochemical and bioelectrocatalytic studies, where reported concentrations are similar or lower than those achieved in this work,[48–50] highlighting the enhanced efficiency of the developed system. This milestone was accompanied by a 1.5-fold increase in the formate synthesis rate (0.66 mM h^{-1} at 1 vvm *vs.* 0.96 mM h^{-1} at 0.1 vvm), indicating enhanced catalytic performance under lower gas flow conditions. Accordingly, this constitutes the highest formate concentration reported to date *via* enzymatic synthesis.

For DHA, its concentration in the medium decreased as the gas volumetric flow rate was reduced (Fig. 4B), however, its low quantification in the liquid phase is attributed to its adsorption onto the biocatalyst with an adsorption capacity of 140.8 mg DHA per g, as previously documented by the authors.[15] This effect arises from strong interactions between DHA and protein amino groups through the Maillard reaction.[51] Compared to the reaction at 1 vvm, which yielded a soluble DHA concentration of 12.2 ± 0.4 mM, the reaction at 0.1 vvm showed only 5.2 ± 0.7 mM, indicating that 92.1% of DHA produced was adsorbed onto the bifunctional biocatalyst (based on the equimolar formate co-production). This behavior may result from changes in the local microenvironment, such as reactor pressure, pH, or dissolved gas concentration, which can shift adsorption equilibria.[52] Despite this significant adsorption, the authors also have reported the saturation of the biocatalyst over several reaction cycles, allowing greater accumulation of DHA in the liquid phase. Likewise, its desorption directly from the biocatalyst has also been demonstrated under mild conditions, achieving desorption yields of up to 27.2 ± 1.8%.[15] However, further studies are needed to clarify the mechanisms driving this DHA adsorption and the contribution of each variable under these conditions.

Regarding glycerol carbonate, its concentration decreased as the gas flow rate was reduced (Fig. 4C). This may result from the multi-enzymatic reaction favoring formate synthesis at lower dissolved CO_2 levels, leading glycerol to be preferentially consumed for DHA production rather than glycerol carbonate synthesis. However, no significant differences were observed in the GC production rate, suggesting that the intrinsic reaction kinetics for this compound were not substantially affected by the gas flow conditions. This indicates that the reaction was not limited by the gas–liquid mass transfer of CO_2. In the case of glycerol, its conversion increased with decreasing gas flow rate, reaching 99.5 ± 1.2% at 0.1 vvm (Fig. 4D). Thus, optimizing reaction conditions can enhance substrate conversion and orientate the system toward improved formate and DHA enzymatic co-production.

Table S2 in SI presents some performance metrics obtained from the three reactions. At 0.1 vvm, a space-time yield (STY) for formate of 37.2 ± 2.2 mg L^{-1} h^{-1} was determined, representing a 1.3-fold improvement compared to the reaction at 1 vvm. A similar improvement was observed in catalyst yield, which reached 29.8 ± 1.7 mg formate per g of biocatalyst. In the case of DHA and GC, these metrics decreased as the volumetric flow rate was reduced due to enhanced DHA adsorption on the biocatalyst and the shift of the reaction conditions to favor the co-production of formate and DHA while minimizing GC formation.

These remarkable findings can also be attributed to the sustained operational stability of the co-immobilized biocatalyst throughout the reaction, as observed in Fig. 5. Notably, enzyme stability increased as the gas flow rate decreased, suggesting reduced inactivation at lower gas flow rate and dissolved CO_2 levels. At 0.1 vvm, GC-GlyDH and FDH retained 80.2 ± 2.1% and 96 ± 1.6% activity after 80 h, representing 1.9- and 1.8-fold improvements over the operational stability of the biocatalyst in the reaction at 1 vvm. This demonstrates the high biocatalyst's robustness and potential for reuse for consecutive reaction cycles under low dissolved CO_2 conditions. In addition, as mentioned earlier, changes in the reaction microenvironment can vary with gas supplementation, affecting parameters such as pH (Fig. S4 in SI). Since pH depends on dissolved CO_2 concentration, this can significantly influence enzyme stability. At slightly acidic pH (6.5–7.0), free GlyDH can lose up to 30% of its activity compared to pH 7.5, whereas free FDH loses only about 10%.[14] Additionally, even when immobilized, the enzymes may show slight pH-dependent inactivation, but much less than in their free form.[53] Consequently, lower dissolved CO_2 helped maintain near-neutral pH, enhancing enzyme stability and biocatalytic efficiency for formate production.

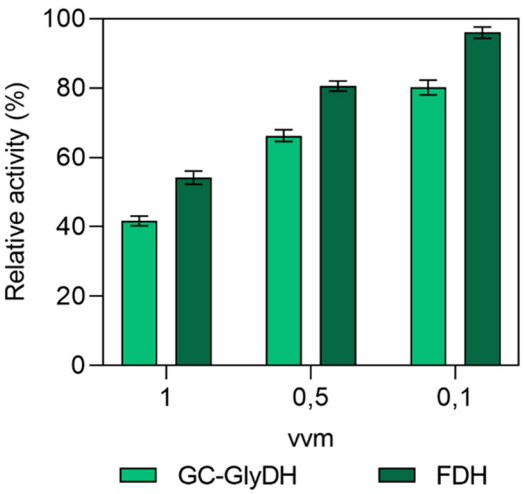

Fig. 5 Operational stability of the bifunctional biocatalyst after 80 h of reaction corresponding to the multi-enzymatic reduction of CO_2 to high-value chemicals by evaluating three different gas volumetric flow rates using a 24% CO_2 gas mixture (1, 0.5 y 0.1 vvm). 100% relative activity was considered as the activity at the initial reaction time (time zero).

3.3. Carbon flow analysis in the CO_2 capture and utilization system

After evaluating the multi-enzymatic system at different gas flow rates, a mass balance was performed to quantify the CO_2 captured and converted, representing the fraction of emissions not released into the atmosphere. The setup included inlet, outlet, and dissolved CO_2 sensors, providing real-time measurements throughout the reaction. Fig. S6 in SI shows the corresponding time-course data. At 1 vvm, dissolved CO_2 concentrations remained stable between 227–247 mg L^{-1} (Fig. S6A), indicating high gas turnover and steady substrate supply. At 0.5 vvm, the maximum CO_2 concentration was ~232 mg L^{-1} but it gradually declined after 50 h, reaching 145 mg L^{-1} by the end of the reaction. A similar behavior was observed at 0.1 vvm, where the maximum CO_2 concentration was only ~214 mg L^{-1}, followed by a steady decline at 48 h and stabilizing during the final two h at around ~36 mg L^{-1}, reflecting a slower gas renewal rate. Despite this, CO_2 remained sufficient to sustain the multi-enzymatic reaction (Fig. S5, SI). Regarding the decline in dissolved CO_2 concentrations observed at 0.5 and 0.1 vvm, it likely reflects CO_2 consumption exceeding gas replenishment, unlike at 1 vvm where renewal maintains stable levels (Fig. 6A).[54] Furthermore, as the reaction proceeds, rising fluid viscosity and foam formation can further limit gas–liquid mass transfer, especially at low gas flow rates.[55]

Regarding the gas inlet and outlet sensors, they operate *via* dual-wavelength infrared (IR) absorption to quantify CO_2 in the gas phase. As shown in Fig. S6B, the inlet CO_2 proportion remained steady at 24.4 ± 0.2%, matching the gas mixture used in all experiments. However, although the inlet CO_2 percentage was the same in all reactions, the actual amount of CO_2 supplied varied with the gas flow rate. At 1 vvm, the outlet CO_2 fraction remained stable at ~21.1 ± 0.1%, indicating ~3.4 ± 0.5% of CO_2 was continuously dissolved into the medium. At 0.5 vvm, the outlet CO_2 was ~19.8 ± 0.9% during the first 30 h, then gradually declined to ~16.4 ± 0.5%, reflecting more CO_2 accumulation in the reaction system over time. At 0.1 vvm, the outlet CO_2 initially increased to ~8.4 ± 0.4% and then steadily decreased after 30 h, reaching complete capture after 55 h, with no CO_2 detected at the system outlet. This behavior reflects lower gas turnover, allowing more efficient CO_2 capture and progressive consumption.

Based on the data collected from the gas sensors, the amount of non-emitted CO_2 (captured fraction) throughout the reaction was determined. Table 1 summarizes the overall CO_2 mass balance, including the amounts of CO_2 supplied, captured, and converted (to formate and/or glycerol carbonate), as well as the yields at each stage. As observed, only 13.8 ± 1.3% of the CO_2 supplied was captured within the system during the reaction conducted at 1 vvm, whereas at 0.5 vvm the CO_2 retention nearly doubled to 24.4 ± 0.9%. This implies that some CO_2 remains in the system, either physically trapped, chemically absorbed (mainly as bicarbonate and other inorganic species), or unconverted due to reaction limitations. In the case of the reaction at 0.1 vvm, an exceptional capture efficiency of 93.3 ± 2.1% was achieved, indicating that the decreased gas–liquid interfacial saturation at low volumetric flow rates resulted in a significant improvement in CO_2 retention within the system for its subsequent conversion. Under these conditions, conversion performance was also favored, where nearly the entire amount of CO_2 captured was converted into the target products, reaching production yields of 0.84 ± 0.07 g of formate and 1.09 ± 0.06 g of GC (as the total molecule) per g of CO_2 captured at 0.1 vvm. Thus, although more CO_2 is captured at 1 vvm, the multi-enzymatic system was favored by the improved biocatalyst performance at near-neutral pH at 0.1 vvm, thereby maximizing the utilization of the captured CO_2. Despite this, the amount of CO_2 converted into products was similar across all reactions, suggesting that conversion is the limiting step of this system.

Based on CO_2 conversion to the target products, Table 2 summarizes key performance metrics for this stage. As observed, enzymatic selectivity for formate increases as the gas flow rate decreases (82.5 ± 2.4% at 0.1 vvm), showing more efficient enzymatic CO_2 utilization at neutral pH. In the case of GC, its non-enzymatic production was less selective, especially at 0.1 vvm, where formate yield was roughly twice that of GC. At 0.1 vvm, all captured CO_2 was efficiently converted into formate and GC, obtaining an overall selectivity of 123.1 ± 2.2%. This apparent overestimation likely arises from the error linked to the determination of captured CO_2 (0.72 ± 0.12 g) which represents almost a 17% of error, combined with the accuracy of the flow meter and gas sensors, particularly when operating at low flow rates. Nonetheless, despite this, the global selectivity in each reaction

Table 1 Material balance and performance metrics for CO_2 capture and conversion in the multi-enzymatic reduction process to high value-added compounds

Volumetric gas flow rate (vvm)	Supplied CO_2 (g)	Captured CO_2 (g)	Capture efficiency (%)	Converted CO_2 [a] (g)	Product yield[b] (g product per g CO_2)	
					Formate	GC
1	7.74 ± 0.23	1.07 ± 0.18	13.8 ± 1.3	0.81 ± 0.13	0.43 ± 0.09	0.90 ± 0.08
0.5	3.87 ± 0.14	0.95 ± 0.08	24.4 ± 0.9	0.84 ± 0.14	0.56 ± 0.04	0.92 ± 0.09
0.1	0.77 ± 0.11	0.72 ± 0.12	93.3 ± 2.1	0.89 ± 0.08	0.84 ± 0.07	1.09 ± 0.06

Experiments were conducted at three different volumetric gas flow rates using a 24% CO_2 gas mixture in a stirred-tank reactor with a 200 mL reaction volume. GC: glycerol carbonate. [a] Corresponding to the fraction of CO_2 atoms incorporated into formate and glycerol carbonate. [b] Based on the total mass of each product.

Table 2 Performance metrics of CO_2 conversion into high-value products, formate and glycerol carbonate (GC), evaluated at different volumetric gas flow rates (1, 0.5 and 0.1 vvm) of a 24% CO_2 gas mixture in a multi-enzymatic system

	Selectivity (%)			
Volumetric gas flow rate (vvm)	Formate	GC	Global process selectivity (%)	Carbon efficiency (%)
1	42.4 ± 1.3	33.5 ± 0.8	75.9 ± 1.1	10.5 ± 0.7
0.5	55.1 ± 1.7	34.4 ± 1.5	89.5 ± 1.6	21.8 ± 1.1
0.1	82.5 ± 2.4	40.6 ± 1.8	123.1 ± 2.2	114.7 ± 1.6

was considerably high, as the system allowed for the maximization of CO_2 utilization to produce both products.

In terms of carbon efficiency, only 10.5 ± 0.7% of the supplemented CO_2 at 1 vvm was converted into the target products (formate and GC), while at 0.5 vvm roughly doubled to 21.8 ± 1.1%. Remarkably, at 0.1 vvm, all supplied CO_2 was converted into the target products (114.7 ± 1.6%), indicating maximal utilization of the total supplemented CO_2. The slight overestimation likely reflects the previously mentioned sources of errors. Under these conditions, glycerol was also almost completely consumed, with a conversion yield of 99.5 ± 1.2% (Fig. 4D). Therefore, the inclusion of an additional CO_2 and glycerol valorization route in this multi-enzymatic system, the synthesis of glycerol carbonate, enhanced the overall carbon efficiency and expanded the products portfolio of this process, thus also contributing to overall process sustainability by generating an additional high-value product from the same feedstocks. Likewise, the potential for developing reactor-scale predictive models based on these operation conditions requires explicit consideration of pH-dependent CO_2 speciation when coupling gas–liquid mass transfer with reaction kinetics. As result, this would enable a more realistic description of CO_2 behavior and availability within the system, ensuring adequate gas supply for the reaction while maximizing conversion efficiency in greener biocatalytic processes.

Several studies have shown successful CO_2 capture and conversion into value-added products. Zhou *et al.* demonstrated the production of methane from CO_2 with complete capture and conversion efficiency (100%) using a fixed-bed reactor packed with adsorbents specifically designed for CO_2.[56] The same reactor, operated in different configurations, has also been widely used to produce various chemicals and fuels from industrial gas streams, achieving capture efficiencies over 85%.[57] On the other hand, CO_2 capture using the regenerative ammonia method has reported efficiencies exceeding 90% for the direct production of fertilizers from CO_2,[58] and capturing CO_2 as carbamic acid from amino acid salts has also been shown to be a feasible strategy for CO_2 utilization to produce compounds such as oxazolidinones.[59] Additionally, among the simplest capture methods, solvent-based approaches have achieved efficiencies above 90% using solvents like monoethanolamine (MEA), 2-amino-2-methyl-1-propanol (AMP), and piperazine (PZ).[60] However, CO_2 conversion in these systems is often limited by solvent degradation, impurities, and the reduced reactivity of CO_2 caused by the formation of stable amine complexes.[61] Finally, although electrochemical systems often achieve high CO_2 conversion rates exceeding 95%, this performance frequently comes at the expense of low selectivity, increased energy requirements and CO_2 supplementation with low capture efficiencies.[62,63]

In the case of enzymatic processes, CO_2 conversion rates are often not reported, mainly due to measurement challenges, the involvement of other inorganic substrates, and the common practice of estimating yields from NADH consumption, as typically done in FDH-catalyzed reactions. However, a study reported a CO_2 conversion to formate efficiency of 80.5% using FDH immobilized on metal–organic frameworks (MOFs), markedly improving the enzyme's catalytic performance.[64] Additionally, complete (100%) conversion of CO_2 from industrial off-gases to formate by FDH was also reported, highlighting the potential of these systems for efficient valorization of gas emissions, even at low CO_2 concentrations.[65] In multi-enzymatic systems, CO_2 reduction has been successfully applied to produce compounds such as pyruvate, achieving conversion of 81%.[66] In contrast, methanol production generally shows much lower CO_2 conversion efficiencies, mainly due to the complexity of multiple sequential enzymatic reduction steps, with reported values ranging from 3% to 25%,[67,68] highlighting the challenges in optimizing these multi-step biocatalytic processes. Finally, carbonic anhydrase has been shown to selectively accelerate CO_2 capture up to 20-fold, while also promoting its conversion into compounds such as carbon monoxide and carbonates, reaching yields of approximately 80% or higher.[6,69] In addition, its synergy with FDH enzymes has been effectively demonstrated to enhance the CO_2 conversion to formate.[46,47] Overall, enzymes represent a feasible biocatalytic tool for the development of sustainable processes aimed at CO_2 capture and conversion into value-added industrial products.

3.4. Environmental implications of the multi-enzymatic CO_2 reduction system

Once the CO_2 conversion performance was evaluated, the environmental impact of these processes was also analyzed. As extensively reported, the enzymatic reduction of CO_2 represents a green and sustainable catalytic route for mitigating greenhouse gas emissions.[70,71] Since enzymes originate from renewable biological systems, they are inherently biocompatible and environmentally benign, offering a safer alternative to heavy-metal and synthetic complex catalysts. Consequently, enzymatic catalysis stands out as a key strategy for advancing carbon-neutral bioprocessing and sustainable industrial chem-

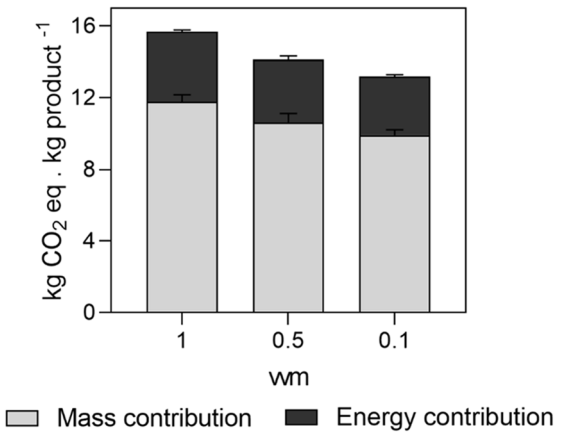

Fig. 6 Total global warming potential (GWP) assessment of the multi-enzymatic reduction of CO_2 to high value-added compounds (accounting for formate, DHA and GC), varying the inlet volumetric gas flow rate from a 24% CO_2 gas mixture.

istry.[72] However, to the best of our knowledge, only few reports have evaluated the environmental impact of these enzymatic processes. Therefore, to evaluate the greenness of this multi-enzymatic reaction, the Global Warming Potential (GWP) was estimated both in terms of the materials used for the production and the energy invested in each reaction carried out at different volumetric gas flow rates (Fig. 6).

A clear correlation was observed between the applied volumetric gas flow rate and the global warming contribution. At the lowest flow rate (0.1 vvm), CO_2 conversion was highest, indicating that maximizing multi-enzymatic carbon utilization can significantly reduce the environmental footprint of the process due to more efficient use of resources. In this reaction, a total GWP of 13.2 ± 0.2 kg CO_2 eq. per kg of product was obtained. Compared to electrochemical CO_2 reduction platforms, some processes can exhibit an environmental impact at least 1.5 times greater than that observed in this study.[73–75] This is mainly due to their high energy consumption, the materials required for electrodes and electrolytes, and their rapid degradability, which generates additional waste. However, in some cases, the optimization of these processes at industrial scales can substantially improve their environmental footprint (up to four times lower than in this study).[76,77] Regarding these enzymatic platforms, information on their environmental performance remains limited; nevertheless, the present study provides a foundational dataset that can be used to further develop a comprehensive Life Cycle Assessment (LCA).

On the other hand, the energy demand and conversion losses associated with fossil-based processes can lead to a higher global warming impact compared to CO_2-based processes, where different amounts of products can be obtained directly from CO_2,[78] as demonstrated in this study. Consequently, renewable-based systems are considered the most promising candidates for achieving negative greenhouse gases (GHG) emissions.[79] As a result, a CO_2 capture and conversion system was successfully developed by investigating the gas–liquid mass transfer of CO_2 and implementing a sensor-based approach to accurately quantify the amount of CO_2 that was prevented from being emitted into the atmosphere and effectively converted into valuable industrial molecules. These findings pave the way for the development of large-scale sustainable multi-enzymatic systems and the establishment of benchmarks such as industrial feedstock valorization, CO_2 capture and conversion efficiency, robust biocatalyst stability, and reduced environmental impact, which could serve as key criteria for identifying promising strategies that make a substantial contribution to GHG mitigation and advance green chemistry and CCU technologies.

4. Conclusions

The gas–liquid transfer of CO_2 in the multi-enzymatic system was successfully evaluated in a stirred-tank reactor using reactor engineering to gain insights into CO_2 mass transfer during the stages of capture and conversion and enabling a first assessment of the sustainability of this type of bioprocess. The volumetric mass transfer coefficient (k_La) was determined with a digital in-line CO_2 sensor based on pH under different gas flow rates from a 24% CO_2 gas mixture, showing that higher flow rates increased CO_2 transfer when the system operated with 10% immobilization carrier resuspended. At the lowest volumetric gas flow rate (0.1 vvm), the multi-enzymatic reaction achieved the highest formate concentration reported to date by an enzymatic route, 66.1 ± 1.4 mM. This was attributed to pH shifts from CO_2 dissolution, which improved biocatalyst stability at near-neutral pH and revealed a strong correlation between pH and CO_2 transfer rate, significantly influencing the biocatalytic transformation. Finally, the mass balance showed that a portion of the supplied CO_2 was effectively retained, avoiding its release to the atmosphere, with the highest capture efficiency at 0.1 vvm (93.3 ± 2.1%). Moreover, although a higher amount of CO_2 was captured at 1 vvm, all CO_2 captured at 0.1 vvm was selectively converted into value-added products (formate and glycerol carbonate) demonstrating the high efficiency of the multi-enzymatic system for CO_2 valorization, facilitated by significantly improved reaction conditions at 0.1 vvm. Thus, evaluating gas flow rate provided key insights into CO_2 gas–liquid transfer, directly enhancing enzyme-driven carbon utilization at low CO_2 concentrations. These insights provide a foundation for further reactor-scale simulations predicting CO_2 behavior based on pH-dependent speciation, mass transfer rates, and other key operating variables under these conditions. Furthermore, the environmental impact assessment highlights enzymatic CO_2 reduction systems as promising and viable strategies for industrial implementation within conventional manufacturing processes, achieving a substantial reduction in the environmental impact of this system, afforded by maximal CO_2 utilization for the production of the target products.

Author contributions

S. R. R. contributed to data curation, formal analysis, investigation and writing the original draft. The project, conceptualized by M. G. and O. R., involved activities such as funding acquisition, project administration, and methodological development. Additionally, M. G. and O. R., were actively engaged in validating, supervising, visualizing, reviewing, and editing this manuscript.

Conflicts of interest

There are no conflicts to declare.

Data availability

All datasets generated or analyzed during this study are available at https://doi.org/10.34810/data2645.

Supplementary information (SI): experimental procedures for the co-immobilization of FDH and GlyDH enzymes, activity assays, protein content measurement, and HPLC analysis. Equations for the response time of the dissolved CO_2 sensor, its operating diagram, and the CO_2 mass balance equations. Scheme of the reaction mechanism for GC formation. Results of the determination of the response time of the dissolved CO_2 sensor, determination of the volumetric mass transfer coefficient (k_La) of CO_2 under different conditions, performances metrics of yields and productivity, pH monitoring, time-course of substrates and products, and monitoring of dissolved CO_2 concentrations and inlet/outlet CO_2 fractions during multienzymatic CO_2 reduction reactions. See DOI: https://doi.org/10.1039/d6gc00387g.

Acknowledgements

S. R. R. acknowledges the Generalitat of Catalunya (AGAUR) for his pre-doctoral scholarship (Joan Oro – 2022FI_B 00955). All the authors acknowledge Generalitat de Catalunya, and the 2021 SGR 00143 and project MEPLAB-CO_2 (TED2021-129732A-I00) funded by MCIN/AEI/10.13039/501100011033 and by the European Union "NextGenerationEU"/PRTR.

References

1 Z. A. Che Ramli, J. Pasupuleti, S. Samidin, W. N. R. Wan Isahak, A. G. N. Sofiah and S. P. Koh, An overview of the conversion technologies of CO_2 into active CO molecule: Reactor engineering, reaction pathways, product purification and upgrading, *Int. J. Hydrogen Energy*, 2025, **157**, 150374, DOI: 10.1016/j.ijhydene.2025.150374.

2 J. Buckingham, T. R. Reina and M. S. Duyar, Recent advances in carbon dioxide capture for process intensification, *Carbon Capture Sci. Technol.*, 2022, **2**, 100031, DOI: 10.1016/j.ccst.2022.100031.

3 J. Lin, Y. Zhang, P. Xu and L. Chen, CO_2 electrolysis: Advances and challenges in electrocatalyst engineering and reactor design, *Mater. Rep.: Energy*, 2023, **3**(2), 100194, DOI: 10.1016/j.matre.2023.100194.

4 O. Ola and M. M. Maroto-Valer, Review of material design and reactor engineering on TiO_2 photocatalysis for CO_2 reduction, *J. Photochem. Photobiol., C*, 2015, **24**, 16–42, DOI: 10.1016/j.jphotochemrev.2015.06.001.

5 X. Ding, W. Liu, J. Zhao, L. Wang and Z. Zou, Photothermal CO_2 Catalysis toward the Synthesis of Solar Fuel: From Material and Reactor Engineering to Techno–Economic Analysis, *Adv. Mater.*, 2025, **37**(2), 2312093, DOI: 10.1002/adma.202312093.

6 S. Talekar, B. H. Jo, J. S. Dordick and J. Kim, Carbonic anhydrase for CO_2 capture, conversion and utilization, *Curr. Opin. Biotechnol*, 2022, **74**, 230–240, DOI: 10.1016/j.copbio.2021.12.003.

7 M. Ndiaye, E. Gadoin and C. Gentric, CO_2 gas–liquid mass transfer and kLa estimation: Numerical investigation in the context of airlift photobioreactor scale-up, *Chem. Eng. Res. Des.*, 2018, **133**, 90–102, DOI: 10.1016/j.cherd.2018.03.001.

8 F. Garcia-Ochoa and E. Gomez, Bioreactor scale-up and oxygen transfer rate in microbial processes: An overview, *Biotechnol. Adv.*, 2009, **27**(2), 153–176, DOI: 10.1016/j.biotechadv.2008.10.006.

9 L. Zhao, H. Y. Hu, A. G. Wu, A. O. Terent'ev, L. N. He and H. R. Li, CO_2 capture and *in situ* conversion to organic molecules, *J. CO2 Util.*, 2024, **82**, 102753, DOI: 10.1016/j.jcou.2024.102753.

10 R. Puskeiler, M. Edler, K. Didzus, R. Müller and J. Gabelsberger, Mass Transfer Considerations for Scale-Up and Scale-Down of Animal Cell Bioprocesses. In: Proceedings of the 21st Annual Meeting of the European Society for Animal Cell Technology (ESACT), Dublin, Ireland, June 7–10, 2009. Dordrecht: Springer Netherlands; 2012. pp. 451–454. DOI: 10.1007/978-94-007-0884-6_77.

11 F. J. Valdés, M. R. Hernández, L. Catalá and A. Marcilla, Estimation of CO_2 stripping/CO_2 microalgae consumption ratios in a bubble column photobioreactor using the analysis of the pH profiles. Application to Nannochloropsis oculata microalgae culture, *Bioresour. Technol.*, 2012, **119**, 1–6, DOI: 10.1016/j.biortech.2012.05.120.

12 J. Walker, Development of Mass Transfer Coefficient Correlations Between Carbon Dioxide and Oxygen for Airlift Devices [All Theses. 4155.] [Internet]. Master of Science Biosystems Engineering. Clemson University; 2023 [cited 2025 Jul 31]. Available from: https://open.clemson.edu/all_theses/4155.

13 A. I. Adnan, M. Y. Ong, S. Nomanbhay and P. L. Show, Determination of Dissolved CO_2 Concentration in Culture Media: Evaluation of pH Value and Mathematical Data, *Processes*, 2020, **8**(11), 1373, DOI: 10.3390/pr8111373.

14 S. R. Rodriguez, G. Álvaro, M. Guillén and O. Romero, Multienzymatic Platform for Coupling a CCU Strategy to

Waste Valorization: CO_2 from the Iron and Steel Industry and Crude Glycerol from Biodiesel Production, *ACS Sustainable Chem. Eng.*, 2025, **13**(4), 1440–1449, DOI: 10.1021/acssuschemeng.4c04908.

15 S. R. Rodriguez, O. Romero and M. Guillén, Enzyme-Powered CO_2 Utilization: A Bifunctional Immobilized Biocatalyst for Intensified CCU of Industrial Feedstocks to High-Value Chemicals, *ACS Sustainable Chem. Eng.*, 2026, **14**(1), 86–98, DOI: 10.1021/acssuschemeng.5c07343.

16 Y. Amao, Formate dehydrogenase for CO_2 utilization and its application, *J. CO2 Util.*, 2018, **26**, 623–641, DOI: 10.1016/j.jcou.2018.06.022.

17 B. Thijs, J. Rongé and J. A. Martens, Matching emerging formic acid synthesis processes with application requirements, *Green Chem.*, 2022, **24**(6), 2287–2295, DOI: 10.1039/D1GC04791D.

18 M. Tomatis, H. K. Jeswani and A. Azapagic, Environmental impacts of valorisation of crude glycerol from biodiesel production – A life cycle perspective, *Waste Manage.*, 2024, **179**, 55–65, DOI: 10.1016/j.wasman.2024.03.005.

19 L. Bricotte, K. Chougrani, V. Alard, V. Ladmiral and S. Caillol, Dihydroxyacetone: A User Guide for a Challenging Bio-Based Synthon, *Molecules*, 2023, **28**(6), 2724, DOI: 10.3390/molecules28062724.

20 S. Lukato, G. N. Kasozi, B. Naziriwo and E. Tebandeke, Glycerol carbonylation with CO_2 to form glycerol carbonate: A review of recent developments and challenges, *Curr. Res. Green Sustainable Chem.*, 2021, 4, DOI: 10.1016/j.crgsc.2021.100199.

21 Y. H. Ke, H. Xu, X. Wang, H. Liu and H. Yuan, Production of glycerol carbonate by coupling glycerol and CO_2 over various metal oxide catalyst, *J. CO2 Util.*, 2024, **83**, 102813, DOI: 10.1016/j.jcou.2024.102813.

22 A. Carceller, M. Guillén and G. Álvaro, Lactic Acid from CO_2: A Carbon Capture and Utilization Strategy Based on a Biocatalytic Approach, *Environ. Sci. Technol.*, 2023, **57**(51), 21727–21735, DOI: 10.1021/acs.est.3c05455, PubMed PMID: 38078668.

23 J. Gao, J. W. Yang, T. Ma, J. Wang, D. Xia, B. Du, *et al.*, Mechanism study on direct synthesis of glycerol carbonate from CO_2 and glycerol over shaped CeO_2 model catalysts, *Chin. Chem. Lett.*, 2023, **34**(12), 108395, DOI: 10.1016/j.cclet.2023.108395.

24 B. Belsa, L. Xia and F. P. García de Arquer, CO_2 Electrolysis Technologies: Bridging the Gap toward Scale-up and Commercialization, *ACS Energy Lett.*, 2024, **9**(9), 4293–4305, DOI: 10.1021/acsenergylett.4c00955.

25 D. J. C. Constable, A. D. Curzons and V. L. Cunningham, Metrics to 'green' chemistry—which are the best?, *Green Chem.*, 2002, **4**(6), 521–527, DOI: 10.1039/B206169B.

26 P. Domínguez de María, General equations to estimate the CO_2 production of (bio)catalytic reactions in early development stages, *RSC Sustainability*, 2024, **2**(12), 3817–3825, DOI: 10.1039/D4SU00535J.

27 M. Kordač and V. Linek, Dynamic measurement of carbon dioxide volumetric mass transfer coefficient in a well-mixed reactor using a pH probe: Analysis of the salt and supersaturation effects, *Ind. Eng. Chem. Res.*, 2008, **47**(4), 1310–1317, DOI: 10.1021/ie0711776.

28 N. Akkarawatkhoosith, W. Nopcharoenkul, A. Kaewchada and A. Jaree, Mass Transfer Correlation and Optimization of Carbon Dioxide Capture in a Microchannel Contactor: A Case of CO_2-Rich Gas, *Energies*, 2020, **13**(20), 5465, DOI: 10.3390/en13205465.

29 F. J. Mojica Prieto and F. J. Millero, The values of pK1 + pK2 for the dissociation of carbonic acid in seawater, *Geochim. Cosmochim. Acta*, 2002, **66**(14), 2529–2540, DOI: 10.1016/S0016-7037(02)00855-4.

30 K. Tsukahara, K. Okamura, T. Noguchi and M. Hatta, Development of an acid extraction-NDIR method for the determination of total dissolved inorganic carbon using small sample volumes, *Galaxea, J. Coral Reef Stud.*, 2025, **27**(1), 62–69, DOI: 10.3755/galaxea.G27O-3.

31 D. Moutafchieva, D. Popova, M. Dimitrova and S. Tchaoushev, Experimental determination of the volumetric mass transfer coefficient, *J. Chem. Technol. Metall.*, 2013, **48**(4), 351–356.

32 D. P. Faasen, F. Sepahi, D. Krug, R. Verzicco, P. Peñas, D. Lohse, *et al.*, Diffusive and convective dissolution of carbon dioxide in a vertical cylindrical cell, *Phys. Rev. Fluids*, 2023, **8**(9), 093501, DOI: 10.1103/PhysRevFluids.8.093501.

33 A. L. Gonçalves, F. Almeida, F. A. Rocha and A. Ferreira, Improving CO_2 mass transfer in microalgal cultures using an oscillatory flow reactor with smooth periodic constrictions, *J. Environ. Chem. Eng.*, 2021, **9**(6), 106505, DOI: 10.1016/j.jece.2021.106505.

34 S. Khajooie, G. Gaus, T. Seemann, B. Ahrens, T. Hua and R. Littke, Exploring Effective Diffusion Coefficients in Water-Saturated Reservoir Rocks via the Pressure Decay Technique: Implications for Underground Hydrogen Storage, *Transp. Porous Media*, 2025, **152**(2), 12, DOI: 10.1007/s11242-024-02148-y.

35 T. F. Aitchison, M. B. Timmons, J. J. Bisogni, R. H. Piedrahita and B. J. Vinci, Using Oxygen Gas Transfer Coefficients to Predict Carbon Dioxide Removal, *Int. J. Recirc. Aquacult.*, 2007, **8**(1), DOI: 10.21061/ijra.v8i1.1416.

36 N. Nickel, J. Fitschen, I. Haase, M. Kuschel, T. W. Schulz, T. Wucherpfennig, *et al.*, Novel sparging strategies to enhance dissolved carbon dioxide stripping in industrial scale stirred tank reactors, *Front. Chem. Eng.*, 2024, 6, DOI: 10.3389/fceng.2024.1470991.

37 S. Nedeltchev, Updated Review on the Available Methods for Measurement and Prediction of the Mass Transfer Coefficients in Bubble Columns, *Fluids*, 2025, **10**(2), 29, DOI: 10.3390/fluids10020029.

38 B. Uyar, M. D. Ali and G. E. O. Uyar, Design parameters comparison of bubble column, airlift and stirred tank photobioreactors for microalgae production, *Bioprocess Biosyst. Eng.*, 2024, **47**(2), 195–209, DOI: 10.1007/s00449-023-02952-8.

39 H. M. Polat, F. M. Coelho, T. J. H. Vlugt, L. F. Mercier Franco, I. N. Tsimpanogiannis and O. A. Moultos, Diffusivity of CO_2 in H_2O: A Review of Experimental Studies and Molecular Simulations in the Bulk and in Confinement, *J. Chem. Eng. Data*, 2024, **69**(10), 3296–3329, DOI: 10.1021/acs.jced.3c00778.

40 I. Antonopoulou, A. de Oliveira Maciel, M. Di Giacomo, M. E. Russo, U. Rova, P. Christakopoulos, *et al.*, Accelerated carbonate weathering by immobilized recombinant carbonic anhydrase, *J. CO2 Util.*, 2025, **94**, 103050, DOI: 10.1016/j.jcou.2025.103050.

41 E. Mohammadian, F. Hadavimoghaddam, M. Kheirollahi, M. Jafari, X. Chenlu and B. Liu, Probing Solubility and pH of CO_2 in aqueous solutions: Implications for CO_2 injection into oceans, *J. CO2 Util.*, 2023, **71**, 102463, DOI: 10.1016/j.jcou.2023.102463.

42 R. Wang, L. Ni, N. Zhang, Q. Li, S. An and L. Wang, Predictive model for CO_2 absorption and mass transfer process based on machine learning methods, *Sep. Purif. Technol.*, 2025, **366**, 132584, DOI: 10.1016/j.seppur.2025.132584.

43 A. Gladis, M. T. Gundersen, R. Neerup, P. L. Fosbøl, J. M. Woodley and N. von Solms, CO_2 mass transfer model for carbonic anhydrase-enhanced aqueous MDEA solutions, *Chem. Eng. J.*, 2018, **335**, 197–208, DOI: 10.1016/j.cej.2017.10.111.

44 Y. Shen, P. Shao, J. Zhao, Y. Lu and S. Zhang, Mass Transfer-Reaction Modeling of CO_2 Capture Mediated by Immobilized Carbonic Anhydrase Enzyme on Multiscale Supporting Structures, *Environ. Sci. Technol.*, 2025, **59**(4), 1995–2005, DOI: 10.1021/acs.est.4c09673.

45 G. Pietricola, T. Tommasi, M. Dosa, E. Camelin, E. Berruto, C. Ottone, *et al.*, Synthesis and characterization of ordered mesoporous silicas for the immobilization of formate dehydrogenase (FDH), *Int. J. Biol. Macromol.*, 2021, **177**, 261–270, DOI: 10.1016/j.ijbiomac.2021.02.114.

46 R. Sato and Y. Amao, Carbonic anhydrase/formate dehydrogenase bienzymatic system for CO_2 capture, utilization and storage, *React. Chem. Eng.*, 2022, **7**(1), 181–191, DOI: 10.1039/D1RE00405K.

47 Y. Li, L. Wen, T. Tan and Y. Lv, Sequential Co-immobilization of Enzymes in Metal-Organic Frameworks for Efficient Biocatalytic Conversion of Adsorbed CO_2 to Formate, *Front. Bioeng. Biotechnol.*, 2019, 7, DOI: 10.3389/fbioe.2019.00394.

48 L. Yan, G. Liu, J. Liu, J. Bai, Y. Li, H. Chen, *et al.*, Hierarchically porous metal organic framework immobilized formate dehydrogenase for enzyme electrocatalytic CO_2 reduction, *Chem. Eng. J.*, 2022, **450**, 138164, DOI: 10.1016/j.cej.2022.138164.

49 S. H. Kim, G. Y. Chung, S. H. Kim, G. Vinothkumar, S. H. Yoon and K. D. Jung, Electrochemical NADH regeneration and electroenzymatic CO_2 reduction on Cu nanorods/glassy carbon electrode prepared by cyclic deposition, *Electrochim. Acta*, 2016, **210**, 837–845, DOI: 10.1016/j.electacta.2016.06.007.

50 D. Maureira, S. R. Rodriguez, O. Romero, M. Guillén, G. Álvaro, L. Wilson, *et al.*, Immobilization of FDH on carbon felt by affinity binding strategy for CO_2 conversion, *Results Eng.*, 2025, **25**, 104442, DOI: 10.1016/j.rineng.2025.104442.

51 Y. Sun, F. A. M. Al-Zahrani and L. Lin, Colour formation of dihydroxyacetone with cysteine and its derivatives via Maillard reaction, *Dyes Pigm.*, 2022, 208, DOI: 10.1016/j.dyepig.2022.110854.

52 M. Wasilewska, A. Derylo-Marczewska and A. W. Marczewski, Comprehensive Studies of Adsorption Equilibrium and Kinetics for Selected Aromatic Organic Compounds on Activated Carbon, *Molecules*, 2024, **29**(9), 2038, DOI: 10.3390/molecules29092038.

53 M. C. Mazzocato and J. C. Jacquier, Recent Advances and Perspectives on Food-Grade Immobilisation Systems for Enzymes, *Foods*, 2024, **13**(13), 2127, DOI: 10.3390/foods13132127.

54 A. B. Gladis, PhD thesis: Upscaling of enzyme enhanced CO_2 capture [Internet], Center for Energy Resources Enginnering. Technical University of Denmark, 2017, [Kongens Lyngby] [cited 2025 Aug 10]. Available from: https://orbit.dtu.dk/en/publications/upscaling-of-enzyme-enhanced-co2-capture.

55 L. Sheng, Y. Chang, J. Deng and G. Luo, Hydrodynamics and mass transfer performance of gas–liquid microflow in viscous liquids, *Chem. Eng. J.*, 2023, **454**, 140407, DOI: 10.1016/j.cej.2022.140407.

56 Z. Zhou, N. Sun, B. Wang, Z. Han, S. Cao, D. Hu, *et al.*, 2D-Layered Ni-MgO-Al_2O_3 Nanosheets for Integrated Capture and Methanation of CO_2, *ChemSusChem*, 2020, **13**(2), 360–368, DOI: 10.1002/cssc.201902828.

57 B. Shao, Y. Zhang, Z. Sun, J. Li, Z. Gao, Z. Xie, *et al.*, CO_2 capture and *in situ* conversion: recent progresses and perspectives, *Green Chem. Eng.*, 2022, **3**(3), 189–198, DOI: 10.1016/j.gce.2021.11.009.

58 L. Fu, Z. Ren, W. Si, Q. Ma, W. Huang, K. Liao, *et al.*, Research progress on CO_2 capture and utilization technology, *J. CO2 Util.*, 2022, **66**, 102260, DOI: 10.1016/j.jcou.2022.102260.

59 A. Liu, R. Ma, C. Song, Z. Yang, A. Yu, Y. Cai, *et al.*, Equimolar CO_2 Capture by N–Substituted Amino Acid Salts and Subsequent Conversion, *Angew. Chem., Int. Ed.*, 2012, **51**(45), 11306–11310, DOI: 10.1002/anie.201205362.

60 Y. M. Chen, H. J. Hsu and Y. J. Lin, Improving CO_2 Capture Efficiency with High-Capacity Solvents: Addressing Temperature-Induced Mass Transfer Limitations, *Ind. Eng. Chem. Res.*, 2025, **64**(4), 2283–2293, DOI: 10.1021/acs.iecr.4c03453.

61 D. Loachamin, J. Casierra, V. Calva, A. Palma-Cando, E. E. Ávila and M. Ricaurte, Amine-Based Solvents and Additives to Improve the CO_2 Capture Processes: A Review, *ChemEngineering*, 2024, **8**(6), 129, DOI: 10.3390/chemengineering8060129.

62 X. Jiang, L. Lin, Y. Rong, R. Li, Q. Jiang, Y. Yang, *et al.*, Boosting CO_2 electroreduction to formate via bismuth

oxide clusters, *Nano Res.*, 2023, **16**(10), 12050–12057, DOI: 10.1007/s12274-022-5073-0.

63 L. Li, A. Ozden, S. Guo, F. P. García de Arquer, C. Wang, M. Zhang, *et al.*, Stable, active CO_2 reduction to formate via redox-modulated stabilization of active sites, *Nat. Commun.*, 2021, **12**(1), 5223, DOI: 10.1038/s41467-021-25573-9.

64 S. Rouf, Y. E. Greish, B. Van der Bruggen and S. Al-Zuhair, Enhancement of CO_2 hydrogenation to formate using formate dehydrogenase immobilized on UiO66 and its derivatives, *Green Synth. Catal.*, 2025, **6**(2), 140–156, DOI: 10.1016/j.gresc.2024.09.005.

65 J. Lee, S. M. Kim, B. W. Jeon, H. W. Hwang, E. G. Poloniataki, J. Kang, *et al.*, Molar-scale formate production via enzymatic hydration of industrial off-gases, *Nat. Chem. Eng.*, 2024, **1**(5), 354–364, DOI: 10.1038/s44286-024-00063-z.

66 M. Miyazaki, M. Shibue, K. Ogino, H. Nakamura and H. Maeda, Enzymatic synthesis of pyruvic acid from acetaldehyde and carbon dioxide, *Chem. Commun.*, 2001, **18**, 1800–1801, DOI: 10.1039/b104873m.

67 S. Sajnani, M. A. Memon, S. A. Memon, A. Kumar, D. Mehvish, S. Ameen, *et al.* CO_2 to Methanol Conversion: A Bibliometric Analysis with Insights into Reaction Mechanisms, and Recent Advances in Catalytic Conversion, *Processes*, 2025, **13**(2), 314, DOI: 10.3390/pr13020314.

68 D. Wang, Y. Du, Z. Liao, X. Hong and S. Zhang, Liquid-phase CO_2 hydrogenation to methanol synthesis: Solvent screening, process design and techno-economic evaluation, *J. CO2 Util.*, 2024, **90**, 102976, DOI: 10.1016/j.jcou.2024.102976.

69 A. G. Fink, E. W. Lees, J. Gingras, E. Madore, S. Fradette, S. A. Jaffer, *et al.*, Electrolytic conversion of carbon capture solutions containing carbonic anhydrase, *J. Inorg. Biochem.*, 2022, **231**, 111782, DOI: 10.1016/j.jinorgbio.2022.111782.

70 R. Villa, S. Nieto, A. Donaire and P. Lozano, Direct Biocatalytic Processes for CO_2 Capture as a Green Tool to Produce Value-Added Chemicals, *Molecules*, 2023, **28**(14), 5520, DOI: 10.3390/molecules28145520.

71 R. A. Sheldon and D. Brady, Green Chemistry, Biocatalysis, and the Chemical Industry of the Future, *ChemSusChem*, 2022, **15**(9), e202102628, DOI: 10.1002/cssc.202102628.

72 L. Yuan, E. M. Bonku and Z. H. Yang, Biocatalysis-driven CO_2 valorization: Innovations and sustainable strategies in conversion and utilization, *Carbon Capture Sci. Technol.*, 2025, **15**, 100437, DOI: 10.1016/j.ccst.2025.100437.

73 L. Ai, S. Ng and W. Ong, A Prospective Life Cycle Assessment of Electrochemical CO_2 Reduction to Selective Formic Acid and Ethylene, *ChemSusChem*, 2022, **15**(19), e202200857, DOI: 10.1002/cssc.202200857.

74 R. Aldaco, I. Butnar, M. Margallo, J. Laso, M. Rumayor, A. Dominguez-Ramos, *et al.*, Bringing value to the chemical industry from capture, storage and use of CO_2: A dynamic LCA of formic acid production, *Sci. Total Environ.*, 2019, **663**, 738–753, DOI: 10.1016/j.scitotenv.2019.01.395.

75 S. J. Blazer, Y. Wang, N. Xu, X. D. Zhou and B. Marchetti, A systematic life cycle assessment of the electroconversion of carbon dioxide, *Sustainable Energy Technol. Assess.*, 2024, **61**, 103574, DOI: 10.1016/j.seta.2023.103574.

76 A. Somoza-Tornos, O. J. Guerra, A. M. Crow, W. A. Smith and B. M. Hodge, Process modeling, techno-economic assessment, and life cycle assessment of the electrochemical reduction of CO_2: a review, *iScience*, 2021, **24**(7), 102813, DOI: 10.1016/j.isci.2021.102813.

77 D. Kang, J. Byun and J. Han, Electrochemical production of formic acid from carbon dioxide: A life cycle assessment study, *J. Environ. Chem. Eng.*, 2021, **9**(5), 106130, DOI: 10.1016/j.jece.2021.106130.

78 A. Sternberg, C. M. Jens and A. Bardow, Life cycle assessment of CO_2-based C1-chemicals, *Green Chem.*, 2017, **19**(9), 2244–2259, DOI: 10.1039/C6GC02852G.

79 N. Badger, D. Mattice, M. Atwood and S. Amini, Life cycle assessment of formic acid synthesis utilizing CO_2 from direct air capture, *RSC Sustainability*, 2025, **3**(5), 2404–2421, DOI: 10.1039/D5SU00111K.